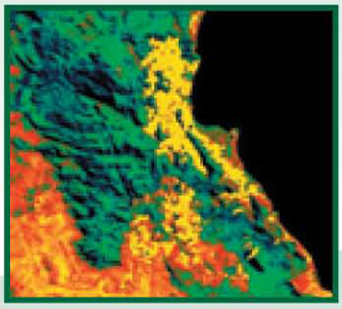

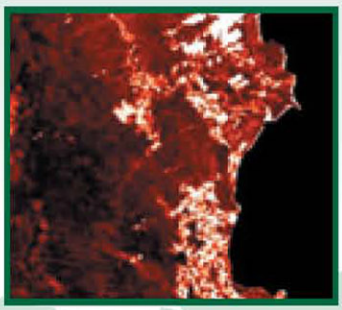

All-weather land-cover change mapping system for the Wet Tropics

Catherine Ticehurst,
Stuart Phinn and Alex Held

Rainforest CRC
Cooperative Research Centre for Tropical Rainforest Ecology and Management

ALL-WEATHER LAND-COVER CHANGE MAPPING SYSTEM FOR THE WET TROPICS

A study on the feasibility of JERS-1 imaging radar for change detection analysis in the Wet Tropics Bioregion of far north Queensland

Catherine Ticehurst,
Stuart Phinn and Alex Held

Rainforest CRC

ISBN 0 86443 692 0

Published by the Cooperative Research Centre for Tropical Rainforest Ecology and Management. Further copies may be requested from the Cooperative Research Centre for Tropical Rainforest Ecology and Management, James Cook University, PO Box 6811 Cairns, QLD, Australia 4870.

This publication should be cited as: Ticehurst, C., Phinn, S., and Held, A., (2003) *All-weather land-cover change mapping system for the Wet Tropics (A study on the feasibility of JERS-1 imaging radar for change detection analysis in the Wet Tropics Bioregion of Far North Queensland).* Cooperative Research Centre for Tropical Rainforest Ecology and Management. Rainforest CRC, Cairns. (28 pp)

March 2003

CONTENTS

ABSTRACT

The aim of this study was to develop a methodology using satellite images collected by a radar system for mapping land cover changes in tropical environments. Radar sensors are "active" imaging systems, providing their own source of illumination and thus can be reliably used in (cloud and smoke prone) tropical environments. For vegetation, radar systems provide information relating to structure, such as height and density of trees.

This study demonstrates the utility of imaging radar data (from the Japanese JERS satellite) as a surrogate for, and add-on to Landsat and aerial photographic imagery in particular for change detection analysis, in the rainforests of the Wet Tropics Bioregion of Far North Queensland. Two important types of change, when examining remotely sensed images of forests, are seasonal change and forest clearing/regrowth. To test how well radar is able to detect land-cover change, Landsat and JERS data sets from two different dates for the Wet Tropics (Daintree River/Cape Tribulation region and Hinchinbrook Island/Tully region) were examined. The results show that imaging radar is able to detect regions of forest clearing as well as seasonal influences on vegetation and land-cover.

DOT-POINT EXECUTIVE SUMMARY

RESEARCH AIM

- Develop a process to map changes in wet–tropics vegetation (especially forest clearing) using radar imagery that can be used under all weather conditions (i.e. through clouds and smoke).
- Monitor the State of the Wet Tropics Environmental Indicator variable "extent of clearing and fragmentation" by using the radar image based mapping.

WHY RADAR IMAGERY

- Radar image data are not affected by cloud cover or smoke, and therefore can be routinely acquired over the entire wet tropics.

POSITIVE FINDINGS

- Using available radar imagery, regions of forest clearing were able to be accurately mapped in a number of sample areas over the wet tropics.
- Radar image data can provide a year round wet-tropics wide vegetation clearing mapping system.
- WTMA has the technology required to perform the data processing.

CONSTRAINTS

- The radar imagery needs to be used in conjunction with existing optical imagery (such as Landsat or SPOT), to establish initial land cover accurately.
- The minimum area of clearing able to be located and verified in this study was 75m by 75m.
- WTMA personnel do not currently have the technical skills required to process radar imagery, although they have the technical equipment (hardware and software).

RECOMMENDATIONS

- The process developed during this research needs to be documented for WTMA and evaluated as an operational mapping method.
- A summary needs to be made of current and future commercially available radar imaging systems (including costs and source) to illustrate the availability of data to be used in this work.

EXECUTIVE SUMMARY

The aim of this study was to develop a robust methodology using satellite images collected by a radar system for mapping land cover changes in tropical environments, which adds value to traditional optical-sensor methodologies for tropical vegetation mapping (e.g. aerial photography and Landsat satellite image data). Radar sensors are "active" imaging systems, providing their own source of illumination and thus can be used in (cloud and smoke prone) tropical environments. In addition, radar systems provide information not normally detectable by optical systems, especially in relation to vegetation structure (height and density of trees).

This project was set up to develop a procedure to primarily monitor the State of Wet Tropics Environmental Indicator variable "extent of clearing and fragmentation" (Phinn *et al.* 2001). An all-weather mapping tool from commercially available image data would be a significant benefit for the environmental capacity of the Wet Tropics Management Authority (WTMA), as it currently relies on aerial photography and rather infrequent passive satellite image data. WTMA has suitable software and base Landsat image data to use the techniques developed in this project, but would require additional training of GIS personnel in the methods used to produce maps from the radar data.

Results from our study show that the JERS-1 imaging radar system, having a certain type of reflected radiation (referred to as L-band, with a wavelength of approx. 25cm) could be used to map changes in some land-cover types, provided earlier Landsat data or existing maps are available to establish original land-cover. The main types of land-cover change that can be mapped from the combined Landsat and imaging radar were:

- Change from rainforest to pasture or low biomass crops; and
- Seasonal dynamics, particularly in woodland or low biomass areas.

The JERS-1 imagery has a raw pixel size of 12.5*12.5 metres. The smallest size of land-cover change detected in our project from this radar imagery, and able to be verified with Landsat, was a region of 75x75 metres (or approximately 6*6 pixels).

Following this study, the recommendations are:

- Imaging radar systems of similar characteristics to JERS-1 are capable of mapping land cover change, however due to its poor signal-to-noise, it is currently recommended as a surrogate for only when optical data (such as Landsat) is unavailable, or to be used in conjunction with optical data to assist in monitoring type of change if needed.

- The use of multi-band, multi-wavelength radar data needs to be further investigated by the authors, to determine its potential applications for the Wet Tropics, not only as a change-detection tool but also for its contribution to existing data layers.

- The process required for change detection analysis using radar should be documented in detail by the authors for potential use by WTMA. This will include radar data availability and costs.

- Imaging radar provides the ONLY all weather imaging system capable of providing regularly updated image maps of the entire wet tropics. A number of operational spaceborne radar systems are currently available for data acquisition, or planned for imminent launch (e.g. Canada – Radarsat; European Union - ERS-2 and ASAR; Japan - JERS-1 and ALOS). At present WTMA does not have the capability to process such types of data. If WTMA is to move towards more operational monitoring using remotely sensed data, and act as an international leader in this area, developing a capacity in Imaging Radar would be advantageous.

INTRODUCTION AND BACKGROUND

Remote sensing has long been identified as an important tool for mapping and monitoring the environment at regional scales. Important environmental indicators applicable to remote sensing technologies have been defined for the Australian Wet Tropics World Heritage Area, to assist in the sustainable management of this region (Phinn *et al.* 2001). Indicators such as land cover, extent of clearing and fragmentation, and structural modifications were identified as being important variables, with remote sensing the only realistic and practical method for their assessment.

While data from the Landsat Thematic Mapper and other passive optical satellite sensor systems are widely used around the world for regional scale analyses (e.g. Skole and Tucker 1993, Archard and Estreguil 1995, Mayaux and Lambin 1997, Lucas *et al.* 2000, Boyd and Duane 2001, Castro *et al.* 2003), the limited availability of cloud free scenes over tropical areas is a significant complication for land-cover change mapping. Synthetic Aperture Radar (SAR) imaging sensors are able to penetrate clouds and haze, enabling frequent and/or routine data acquisition in regions of consistently high cloud cover and areas with extensive smoke and haze cover. The Japanese Earth Resource Satellite (JERS-1), an L-band radar satellite which operated between 1992-1998, has been used for rainforest mapping over extensive areas of South America, Central Africa and South East Asia (Rosenqvist *et al.* 2000), but to date it had not been used to map tropical rainforests in Australia. The long wavelength of this L-band radar system (approx. 25cm in wavelength) is especially advantageous as it penetrates more deeply into dense vegetation and provides information on the structural characteristics and moisture content of different vegetation types (e.g. Lucas *et al.* 2002). L-band radar is also better at discriminating between forests and cleared areas in regions of high biomass compared to the 3-7cm C-band SARs. A detailed introduction to imaging radar is provided in the attached document (Appendix A).

This study demonstrates the utility of imaging radar data (from the Japanese JERS satellite) as a surrogate for, and add-on to Landsat and aerial photographic imagery in particular for change detection analysis, in the rainforests of the Wet Tropics Bioregion of Far North Queensland. Although JERS is no longer operating, other radar satellites have been launched (Envisat's ASAR – C band) and more are scheduled for launch in the next few years (e.g. Radarsat 2 – C band, ALOS's Palsar – L band).

The two major types of change of interest, and which are able to be mapped by both SAR and Landsat, are clearing/regrowth and the more subtle seasonal change. Selective logging has also been reported as being able to be mapped from SAR data, however this was not considered to be a major source of change in the Wet Tropics and, hence not demonstrated here.

Two important factors which influence the response of vegetation to the radar microwaves, and which should be considered when interpreting differences seen in radar images, are the effects due to differences in vegetation structure/biomass and those which might be caused by differences in moisture content in the soil and vegetation. An increase in moisture content in the vegetation and especially soil will reduce radar penetration, often resulting in an increase in backscatter (French *et al.* 1996, Griffiths and Wooding 1996). While flat open areas will have a low backscatter due to specular scattering of the microwaves away from the receiver ['specular scattering'] (Figure 1), trees tend to act as strong reflectors causing the microwaves to bounce off the ground and then their trunks, before returning a signal to the receiver ['double bounce']. In many cases, the radar microwaves also get scattered inside the tree canopies before returning to the receiver ['volume scattering']. Volume scattering tends to dominate in dense forests where less radar signal is able to reach the ground. Conversely double bounce dominates in more open forests. As a result, cleared

areas tend to show up in radar imagery as patches of reduced backscatter. Radar backscatter has thus been shown to correlate with above-ground biomass (e.g. Kasischke *et al.* 1995, Luckman *et al.* 1997, Saatchi and Moghaddam 2000, Castro *et al.* 2003). These differences are therefore exploited in the analysis of images containing open fields and dense forests. Incidence angle and topography will also influence the backscatter response, however these factors will not change with time.

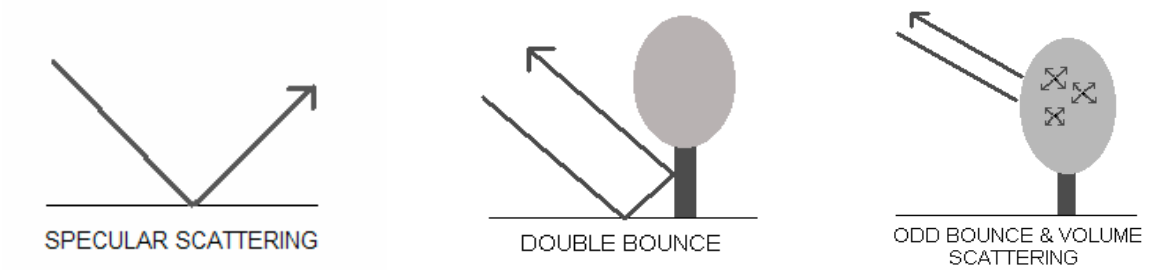

Figure 1: The arrow indicates the three main interactions characteristic of the path of incident radiation from the radar transmitter and then scattered back to the radar sensor.

The more subtle structural and moisture-content seasonal changes are seen in rainforests as well as agricultural vegetation. Topography in the wet tropics has an influence on local climate and soil types, and hence also correlates to the presence of different forest types, including the abundance of deciduous trees (Webb 1968). This later characteristic [abundance of deciduous species], makes the use of radar for seasonal-change or drought detection in forests quite appealing.

Sugarcane is a dominant crop in far north Queensland (FNQ), usually harvested between July and September. Cleared paddocks, after harvesting, will have a smaller backscatter intensity compared to mature crops due to different biomass levels (e.g. Ferrazzoli *et al.* 1997, Hill *et al.* 1999). However, its effect depends on local crop rotation cycles and whether the paddocks are cleared of remnant stubble.

METHODOLOGY

In order to test how well radar is able to detect land-cover change, an experiment was performed with Landsat and JERS data on two sets of images from the Wet Tropics: (1) the Daintree River/Cape Tribulation region, where most of the rainforest is heritage protected; and (2), Hinchinbrook Island/Tully region, where some of the rainforest is privately owned and under pressure for clearing in coastal areas adjacent to sugar cane farms. These data acquisition dates are shown in Table 1.

Table 1: Acquisition dates of existing Landsat and JERS imagery for the Daintree River/Cape Tribulation and Hinchinbrook Island/Tully region of Far North Queensland.

Daintree / Cape Tribulation		Hinchinbrook Island / Tulley	
Landsat	JERS	Landsat	JERS
September 1988			
June 1994	December 1995	September 1994	January 1994
September 1999	June 1996	August 1999	July 1996

Landsat Thematic Mapper (TM) and Enhanced Thematic Mapper (ETM) data (25m pixel size) for path/row 96/71 (covering the Daintree/Cape Tribulation region) was available for September 1988 (TM), June 1994 (TM), and September 1999 (ETM). The JERS scenes (12.5m pixel size) covering the same area were acquired in December 1995 and June 1996. For the Tully region Landsat scenes (path/row 95/73) were available for September 1994 and August 1999, while two JERS scenes were acquired in January 1994 and July 1996. Unfortunately the Landsat scenes did not coincide with the season/year of the JERS scenes, instead the closest matching dates were used.

For remotely sensed images to be compared, geometric (spatial) and radiometric (brightness) differences had to be considered. For the JERS scenes, the spatial offset between them needs to be accounted for. First the JERS scenes were rotated by 90 degrees clockwise so that north was in approximately the correct position. Since each JERS scene in a pair covered a slightly different extent, they were registered together by determining an offset and subsetting the scenes to match. The radar images were then smoothed using a gamma filter, designed to reduce speckle in the image, whilst maintaining edges. These images did not need correction for topographic distortion since they are both subject to a similar level of geometric and radiometric distortion.

In the Landsat data, a dark-pixel subtraction was applied to each image for relative calibration, where the lowest Digital Number (DN) for each band is subtracted from all the pixels of that band (Lu *et al.* 2002). The Landsat scenes covering the same areas were also registered together by determining an offset and subsetting the scenes to match. Subsequently, the Normalized Different Vegetation Index (NDVI) was calculated for each of the images for the change-detection process. This index utilizes the relationship between the red and near-infrared regions of the spectrum and is correlated to vegetation's green leaf cover (Tucker 1979).

For the JERS and Landsat scenes to be compared, the images had to be geo-located and of the same pixel size. This was achieved by warping or registering the JERS scenes to the Landsat scenes. Topographic distortions in the JERS scenes were not corrected since this

would be time consuming and unnecessary for this study, and instead only the flatter regions were used to collect Ground Control Points (GCPs) for warping. For an initial iteration, 20-30 GCPs were located on JERS and Landsat scenes, before the JERS was warped applying a 2nd order polynomial nearest neighbour routine. Using this new JERS scene as a guide, an additional set of 10-15 points were then collected in regions where the match between the warped JERS and Landsat was found to be poor. Following a second iteration warping, a set of difference images (i.e. one scene subtracted from the other) were created for the JERS data and the Landsat data (Figure 2).

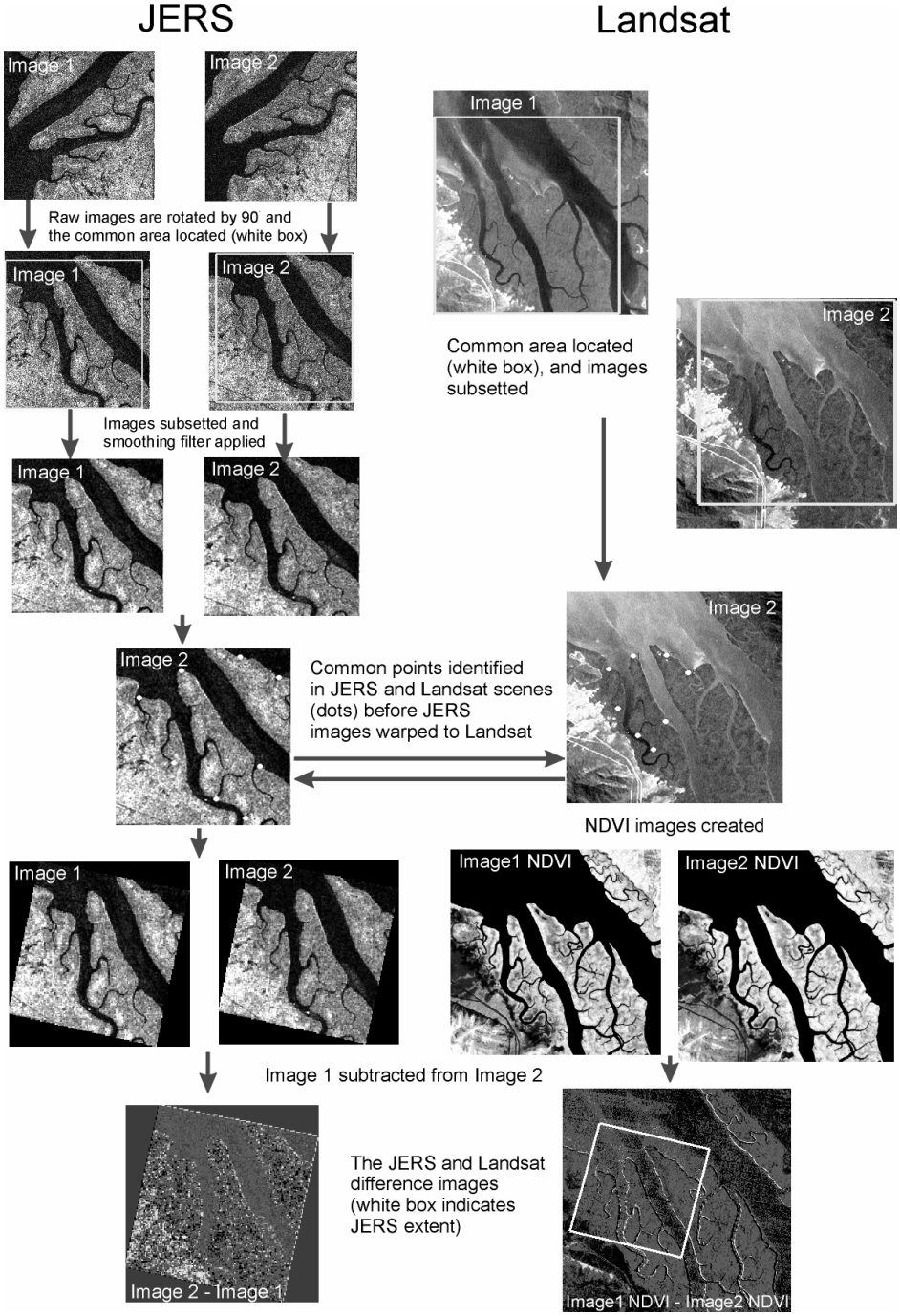

Figure 2. Flowchart of the preliminary processing of JERS and Landsat imagery. For seasonal changes, image 1 and image 2 are from different seasons. Image 1 should be from the same season in both the JERS and Landsat imagery, with image 2 from the same season in both JERS and Landsat imagery. For forest clearing and regrowth detection, image 1 should be an earlier acquisition than image 2. Image 1 should be from a similar date in both the JERS and Landsat imagery, as should image 2.

Note that matching the JERS pairs is very important since the pixel size increases from 12.5m to 25m following warping, hence small changes will be lost in the JERS difference image unless the match is accurate. However, the match between the Landsat and JERS scenes need only be accurate enough to identify equivalent regions.

Two important types of change, when examining difference images of forests, are seasonal change and forest clearing/regrowth. Figure 3 illustrates how forest clearing is visible in both the JERS and Landsat imagery. Although detection of the latter is desired for forest management, the seasonal component also needs to be addressed.

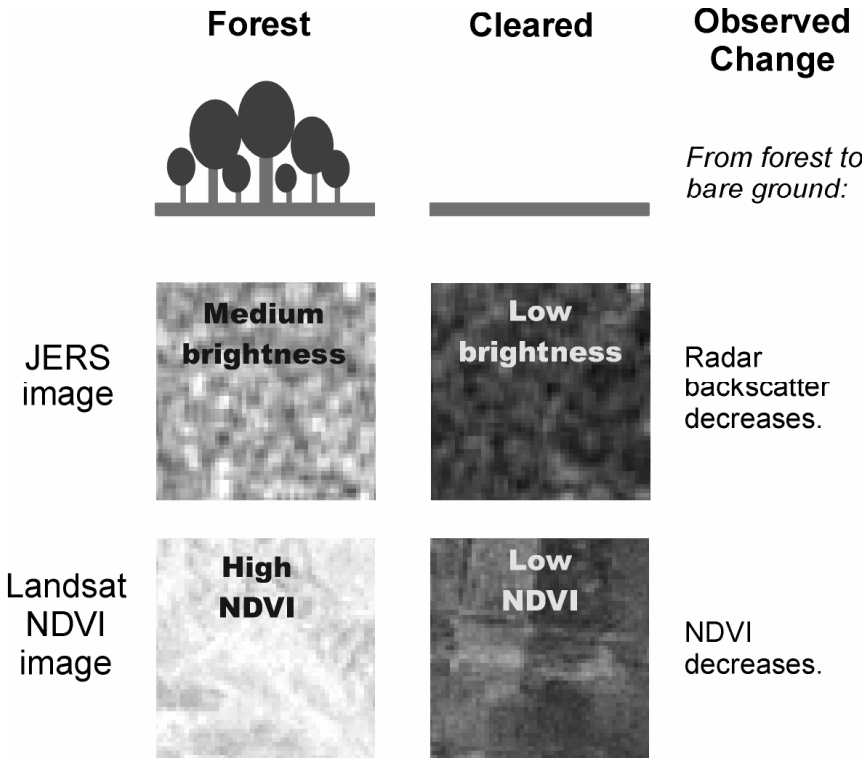

Figure 3. An example of the changes observed in JERS and Landsat imagery when forest clearing occurs

RESULTS

The results have been separated into two types of change **(1) seasonal change** (using the Daintree/Cape Tribulation scenes) and **(2) clearing/regrowth change** (using the Hinchinbrook Island/Tully scenes). The Hinchinbrook Island/Tully Landsat data were from the same time of year, so seasonal information could not be verified, however a number of chronological changes were found, including a reduction in forest extent, which could be tested on the JERS scenes.

SEASONAL CHANGE: *(DAINTREE/CAPE TRIBULATION)*

For this analysis, the Landsat scene from 1999 and JERS scene from 1996 (Figures 4 and 5, respectively) are used as the baseline. For reference, the Tracey and Webb map is also shown as a guide to land cover types (Figure 6).

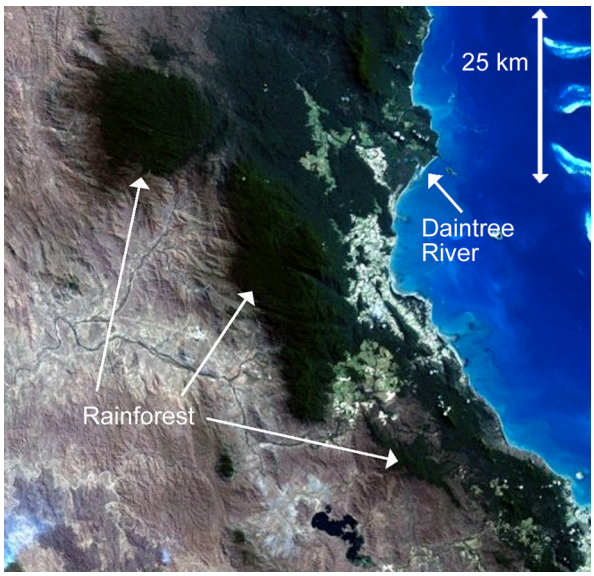

Figure 4. True colour Landsat 7 scene (1999) of the Daintree River / Cape Tribulation region. The dark green regions are rainforest, brown is woodlands and white is agriculture.

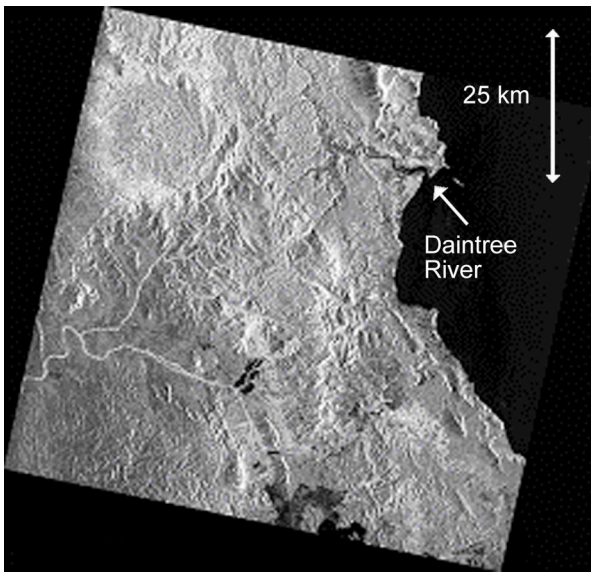

Figure 5. JERS scene [gamma filtered] (1996) of the Daintree River / Cape Tribulation region covering the same extent as Figure 4.

A difference image was calculated by subtracting the pixel values of the December 1995 JERS scene from the June 1996 scene (Figure 7). Hence, a positive value (brighter area) indicates an increase in backscatter from the summer to winter season. For direct seasonal comparison to the JERS images, the Landsat 1999 NDVI (spring) scene was subtracted from the 1994 NDVI (winter) image (Figure 8). Unfortunately due to excessive cloud cover, no summer Landsat scenes were available at the exact period of the JERS images.

To assess how much of the observed change in the optical data was caused by seasonal factors, the September 1999 NDVI scene was also subtracted from an equivalent dry-season September 1988 NDVI scene for comparison. The difference images (in absolute value) for the September 1988 minus September 1999 image, and the June 1994 minus September 1999 images are shown in Figures 9 and 10 respectively. The absolute value was used to allow for better change/non-change discrimination, compared to the standard difference image which is more indicative of type of change. Ignoring cloud effects in the top right corner of Figure 9, there is greater difference in NDVI in the winter'94-spring'99 image than the spring'88-spring'99 image.

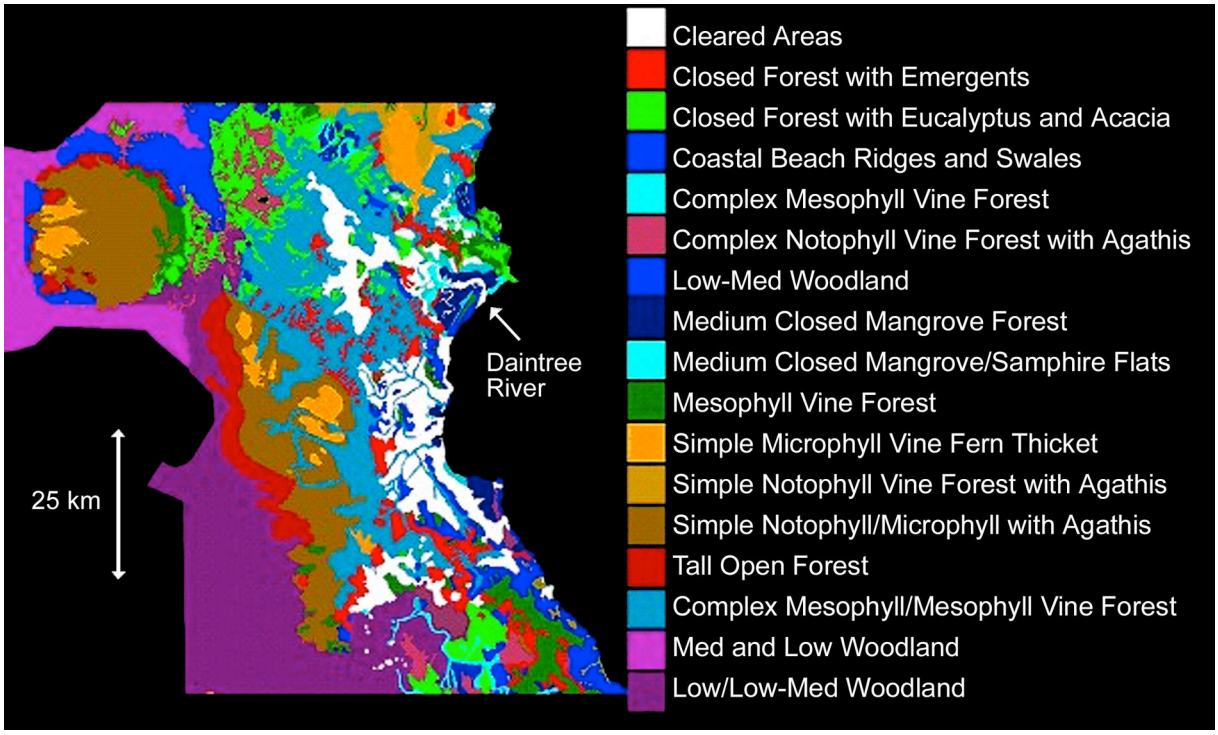

Figure 6. Tracey and Webb classification map of the same regions as Figures 4 and 5.

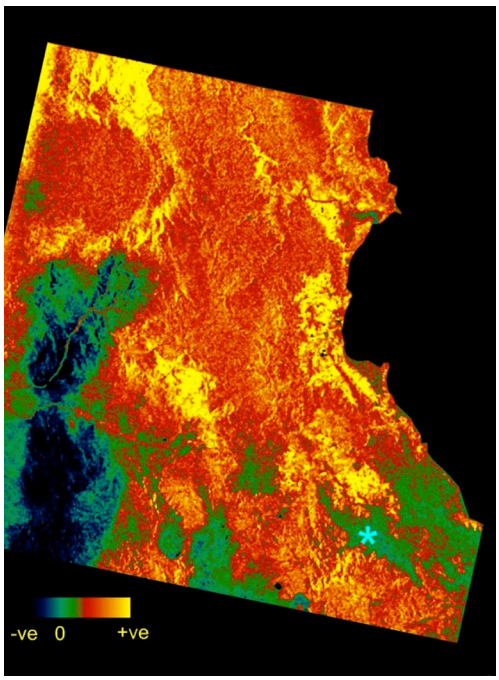

Figure 7. Backscatter difference image — JERS 1996 (winter) — JERS 1995 (summer). Asterisk shows rainforest with negative change. Blue/green colours indicate a reduction in backscatter from summer to winter, while red/yellow shows an increase.

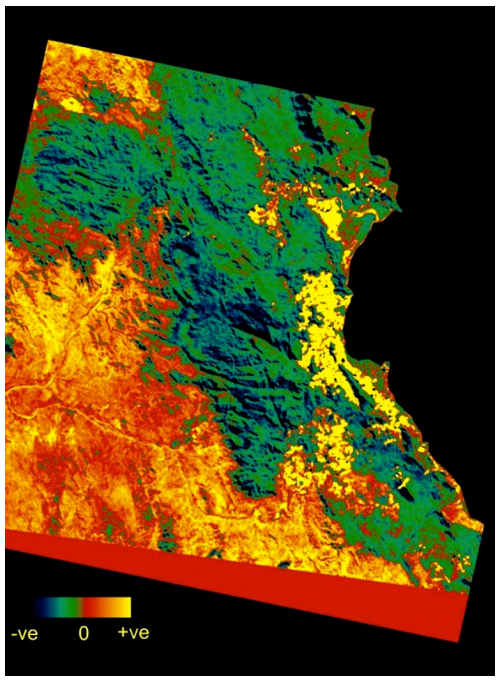

Figure 8. NDVI difference image: 1994 (winter) — 1999 (spring), covering the same extent as Figure 7. Blue/ green indicates a reduction in greenness from spring to winter, while red/yellow shows an increase. Bright yellow regions (right) are agriculture and blue/green is rainforest.

Expected changes between the spring'88-spring'99 images occurred in the agricultural areas (shown as bright in Figure 9). In addition, some change was also observed in the woodland region along the bottom of the image. The seasonal changes in the woodland region were

much more extensive in the winter'94-spring'99 difference image, as well as the rainforest regions which have no significant change in the spring'88-spring'99 scene. This reinforces the notion that seasonal changes in this region are greater than chronological changes due to clearing/regrowth, naturally with the exception of agricultural zones.

From the seasonal change images for the JERS (Figure 7) and Landsat scenes (Figure 8), it is immediately obvious that the JERS image has a very dark region in the southwest corner, which is not visible in the corresponding Landsat scene. This region shows a reduction in backscatter of ~1000 DN, corresponding to from –8.8 dB to –10.2 dB in radar radiometric units [for JERS-1, $dB=20*\log_{10}(\text{raw DN}) - 85.34$ (Shimada 1998, Rosenqvist personal comm. 2001)]. Inspection of an NDVI image (Figure 11) reveals that this region contains a very low NDVI (around 0.1) corresponding to low/low-medium woodlands in the Tracey and Webb map (Figure 6). One factor which could show this effect would be due to an increase in seasonal rainfall, promoting growth of vegetation and hence an increase in biomass and radar backscatter. Furthermore, radar's sensitivity to soil and vegetation moisture content, which increases the dielectric constant of the material, will most likely lead to an increase in the observed backscatter. However, this is speculation as it cannot be verified without Landsat imagery from the same dates as the JERS acquisitions.

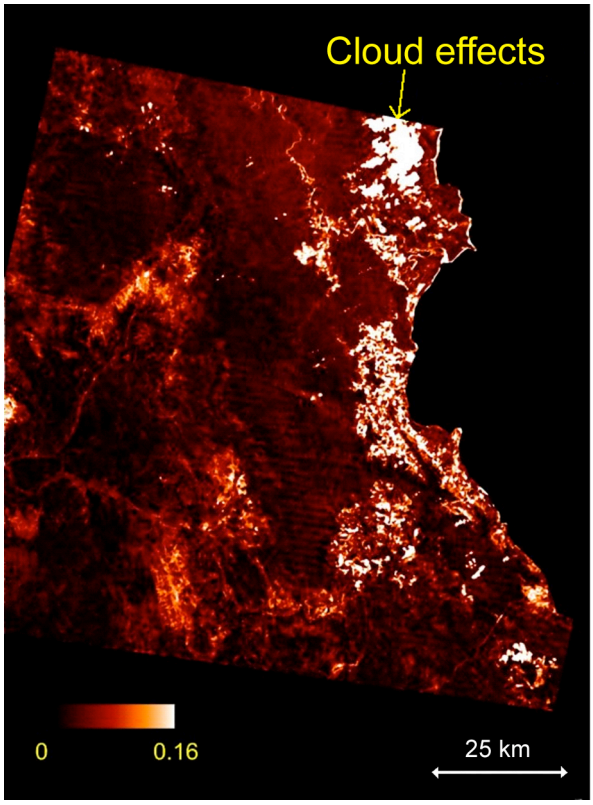

Figure 9. Absolute NDVI difference image: 1998 (spring) — 1999 (spring), covering the same extent as Figures 7 and 8. Dark represents no change, white represents maximum detected change.

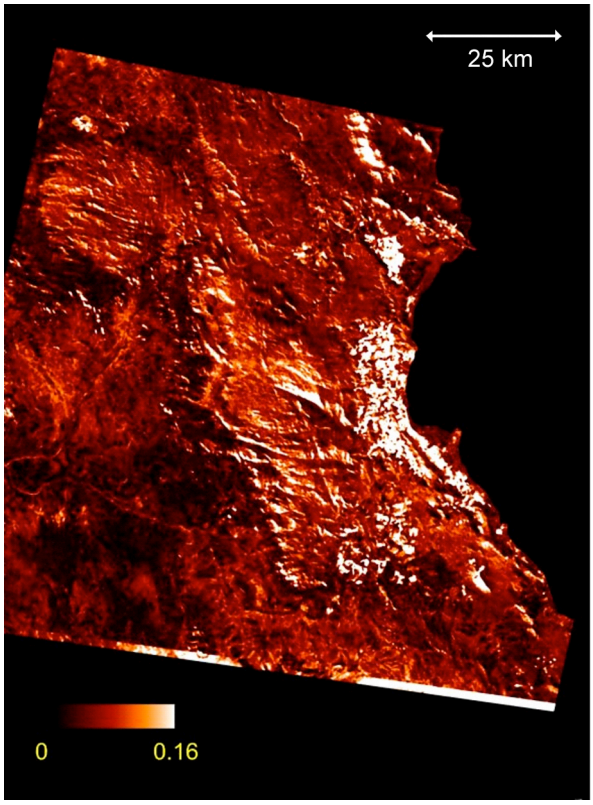

Figure 10. Absolute NDVI difference image: 1994 (winter) — 1999 (spring), covering the same extent as Figures 7, 8 and 9. Dark represents no change, white represents maximum detected change. Image is scaled the same as Figure 9 so the colours are comparable between figures.

Another discrepancy was observed between the Landsat and radar difference images in rainforest areas (showing as blue/green in Figure 8). Although only small in magnitude, there is an overall increase in backscatter (of approximately 1250 DN or from –9.3 dB to –7.7 dB) from summer to winter for most of the rainforest in the JERS image, and a decrease in NDVI (of –0.08) from spring to winter in the Landsat scene. This is possibly due to the influence of the wet season that usually arrives during late spring. Rainfall also increases the dielectric

constant of the scattering materials, which in turn could increase backscatter. To test whether the 1999 spring was unusual for the season, the 1988 NDVI spring image was also subtracted from the 1994 NDVI winter image. There was still a reduction in rainforest NDVI (of –0.095) from spring to winter.

There is, however, a section of the rainforest (marked by the cyan '*' in Figure 7) that has an average decrease in radar backscatter from summer to winter. Reasons for this portion of rainforest being different to the remaining rainforest are unknown, however the Landsat seasonal difference image winter'94-spring'99 (Figure 8) has a slightly smaller reduction in NDVI (an average of –0.06) for this region of rainforest compared to the remaining rainforest (-0.1 NDVI difference). Inspection of the individual winter and spring NDVI scenes shows the variation in the difference image comes from the winter image, where the average NDVI is around 0.52 for the dark rainforest (marked with a '*' in Figure 7), compared to the remaining rainforest with an average NDVI of 0.48. The spring NDVI image shows all rainforest regions to be around 0.58.

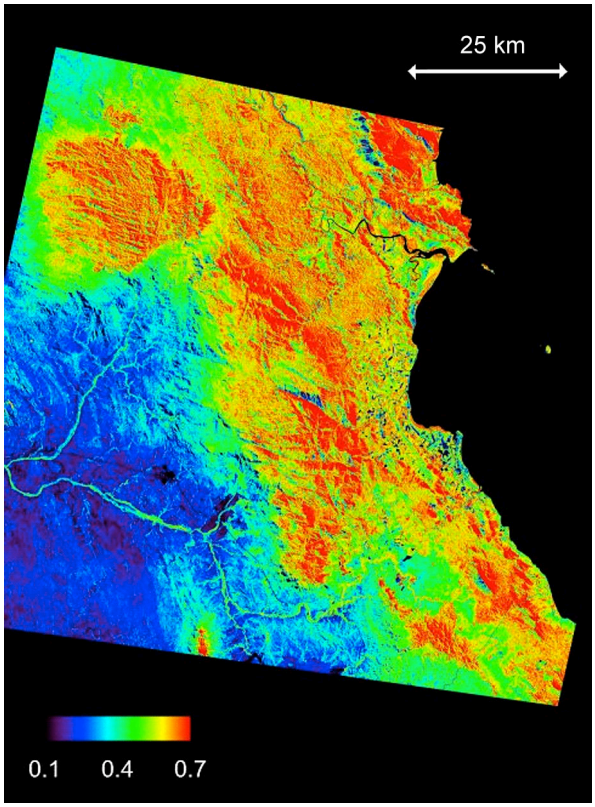

Figure 11. NDVI image for June 1994. Blue represents low NDVI, green is medium NDVI and red is high NDVI.

Apart from some observed anomalies, there were some visible correlations between the JERS and Landsat seasonal difference images. The woodlands, with the exception of the low-NDVI southwest corner, showed a general increase in backscatter from summer to winter for the JERS data and an increase in NDVI from spring to winter for the Landsat data. This indicates an increase in vegetation biomass in both the JERS and Landsat scenes. The agricultural regions showed a large positive increase (i.e. white) in both the radar and NDVI scenes.

CLEARING/REGROWTH CHANGES: *(HINCHINBROOK ISLAND/TULLY)*

In L-band radar imagery, backscatter intensity observed from rainforests is generally higher than from open pastures and crops. Therefore a decrease in backscatter from the earlier scene to the later scene would suggest a reduction in vegetation structure and cover. To ascertain that such changes did occur in this region, an early Landsat scene was used as an initial guide. The NDVI was used from the earlier scene to show regions where vegetation exists, however caution is required since this will also include agricultural areas of high green biomass.

One of the main advantages in using SAR for change detection is that these data are more sensitive to changes in vegetation structure rather than 'greenness' in vegetation. A good example is observed when a rainforest is cleared and replaced by dense pasture. In optical data, the NDVI may not have changed considerably (Figure 12b), however the difference

was readily detected with radar over the same area (Figure. 12c) due to the different scattering caused by the different vegetation structure. One disadvantage, however is that radar can not separate the minor colour differences in recently cleared areas where vegetation cover is still low (white in Figure 12a) from the open pastures.

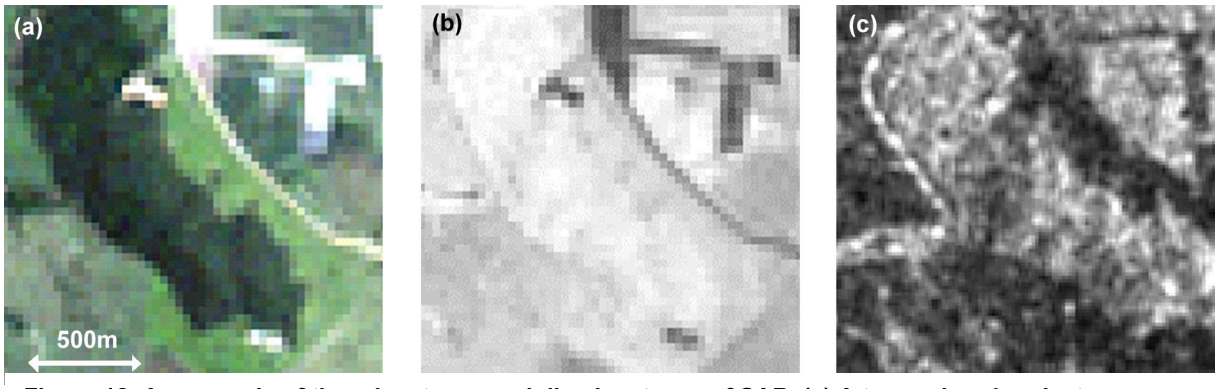

Figure 12. An example of the advantages and disadvantages of SAR. (a) A true colour Landsat scene. (b) An NDVI image of the same scene. (c) A JERS image of the same region. The difference between the forest (dark green in 12a) and pasture (light green in 12a) is more obvious in the JERS image (12c) than in the NDVI image (12b).

While there was a discrepancy in acquisition dates for the JERS and Landsat scenes, changes that occurred between September 1994 and July 1996 were comparable in both data pairs. The significant gap between the latest JERS scene (1996) (Figure 14) and the latest Landsat scene (1999) (Figure 13), meant that some changes in the Landsat pair were not visible in the radar data. For reference, the Tracey and Webb map is also shown as a guide to land cover types (Figure 15). Like in the analysis of the Daintree scenes, some seasonal changes were apparent in the JERS difference images. Thus seasonal change must be considered when assessing whether changes are permanent.

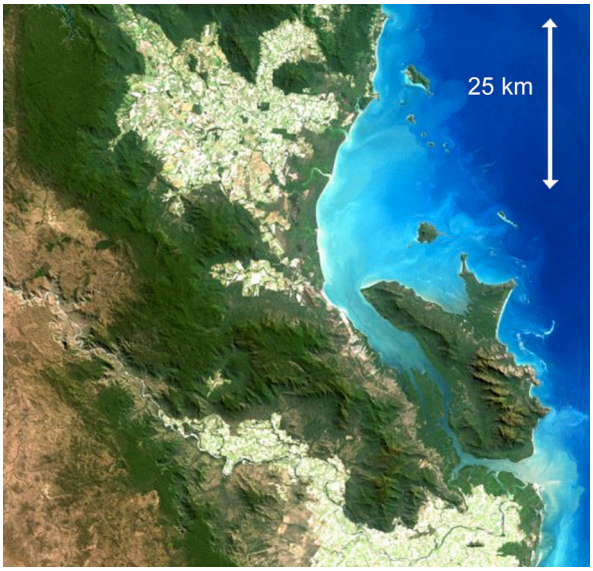

Figure 13. True colour Landsat 7 scene (1999) of the Hinchinbrook/Tully region. The dark green regions are rainforest, brown is woodlands and white is agriculture

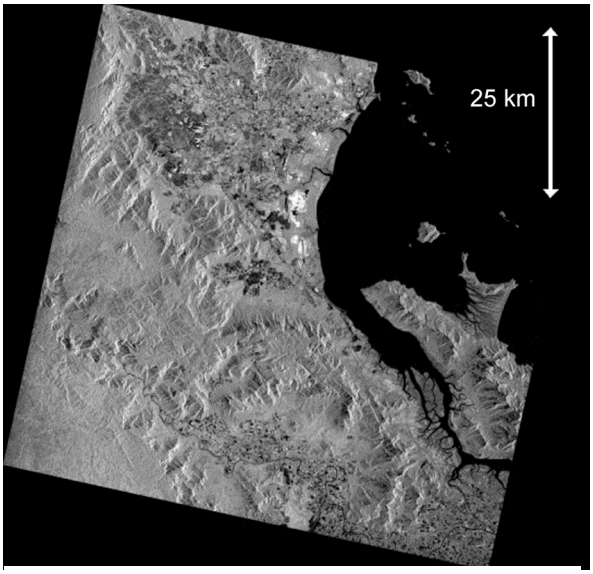

Figure 14. JERS scene [gamma filtered] (1996) of the Hinchinbrook/Tully region covering the same extent as Figure 13.

Since rainforest clearing is expected to be very small for this protected tropical region, an automatic segmentation (or clustering) algorithm was applied to the JERS difference image. This algorithm requires the user to define a minimum and maximum digital number threshold, along with a minimum number of pixels required for a segment to form. We therefore chose to use a range between –5000 to –2000 DN, to make apparent only large

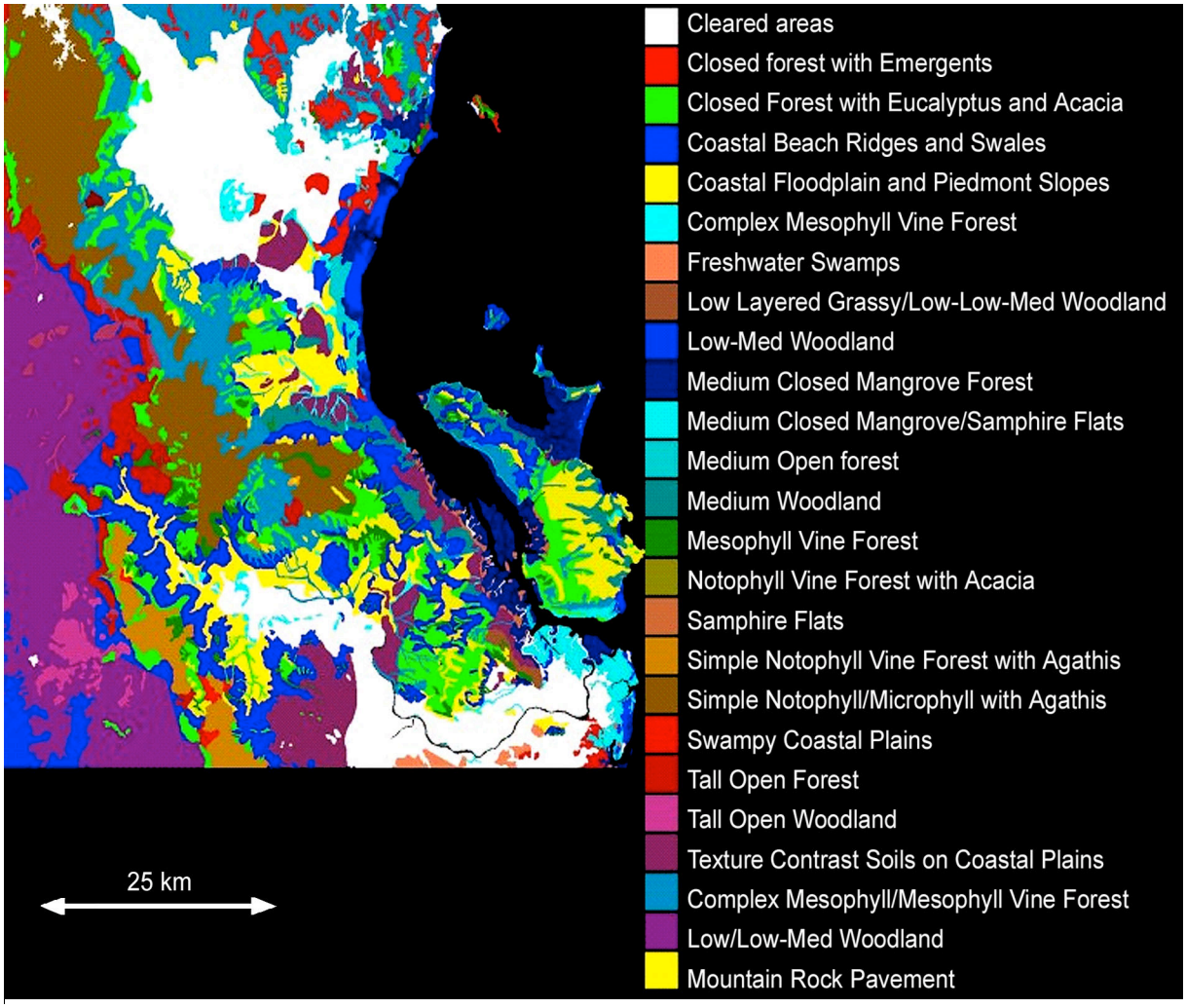

Figure 15. Tracey and Webb classification map of the same region as Figures 13 and 14.

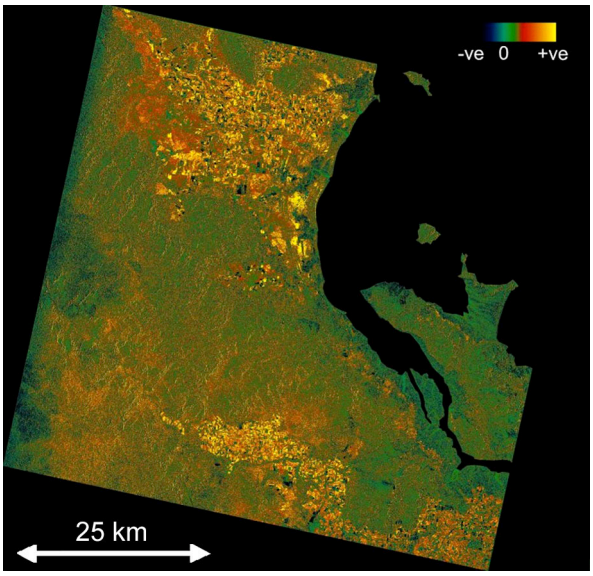

Figure 16. Backscatter difference image: JERS 1996 (winter) - JERS 1994 (summer). Blue/green colour indicates a reduction in backscatter while red/yellow shows increase.

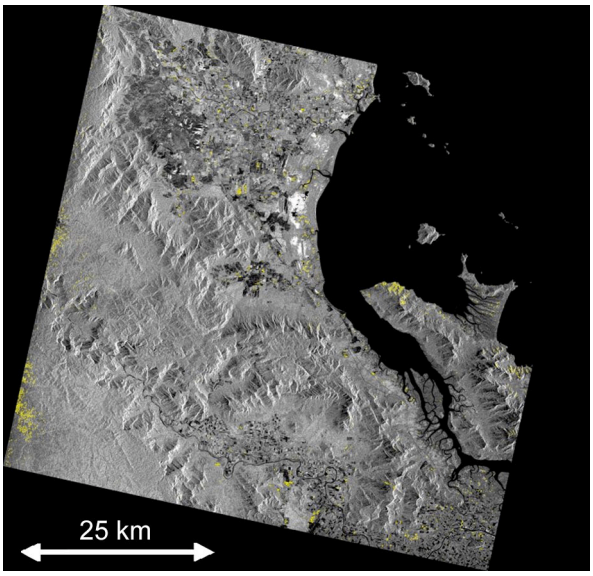

Figure 17. 1996 JERS scene [gamma filered] with the extracted change-detection segments shown in yellow.

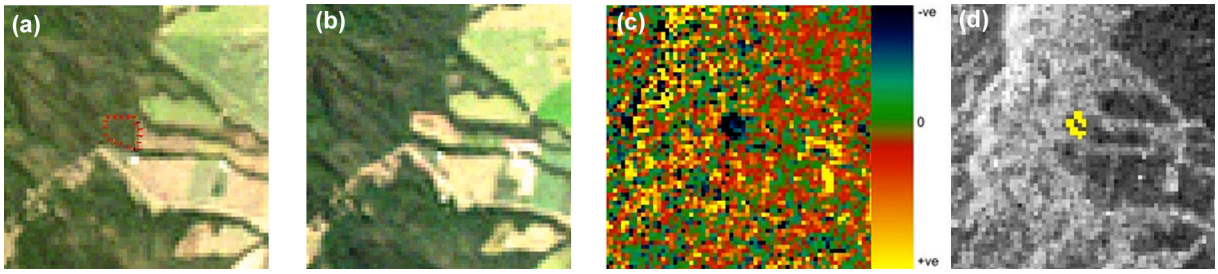

Figure 18. An example of a small patch of deforestation that is visible in Landsat and JERS imagery. (a) Landsat 1994 – the removed forest is shown in red, and (b) 1999 Landsat Image. (c) A JERS difference image, and (d) change segmentations (yellow) overlaid on the 1996 JERS band.

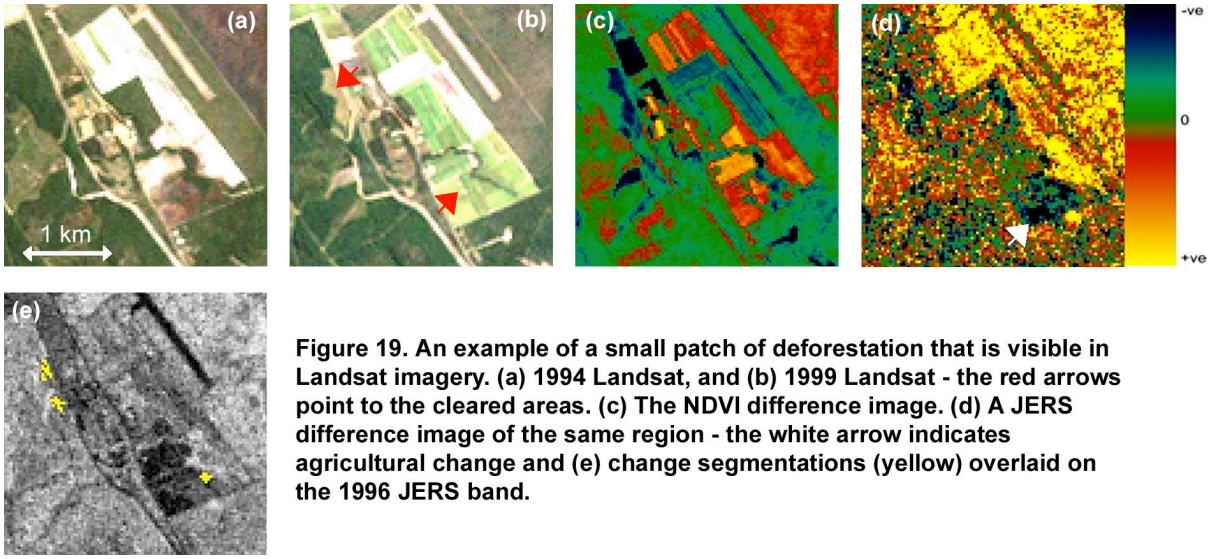

Figure 19. An example of a small patch of deforestation that is visible in Landsat imagery. (a) 1994 Landsat, and (b) 1999 Landsat - the red arrows point to the cleared areas. (c) The NDVI difference image. (d) A JERS difference image of the same region - the white arrow indicates agricultural change and (e) change segmentations (yellow) overlaid on the 1996 JERS band.

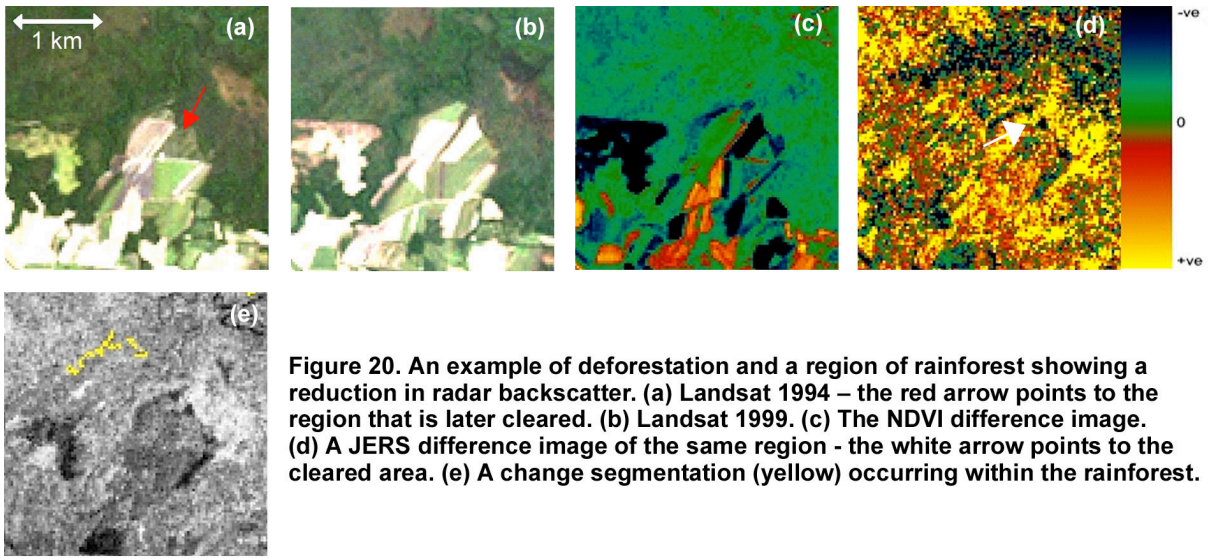

Figure 20. An example of deforestation and a region of rainforest showing a reduction in radar backscatter. (a) Landsat 1994 – the red arrow points to the region that is later cleared. (b) Landsat 1999. (c) The NDVI difference image. (d) A JERS difference image of the same region - the white arrow points to the cleared area. (e) A change segmentation (yellow) occurring within the rainforest.

reductions in backscatter, with a minimum segment size of 15 pixels (kept small to extract small deforestation sites). Note that this automated segmentation step is not essential for investigating small changes. An alternative method would be to create a mask of the image using the same threshold, and visually locating regions where “clumps” appear to form. This is more time consuming, however it also prevents small but possibly important regions from being omitted.

The JERS difference image is shown in Figure 16, while the resultant segments overlaid on the image are shown in Figure 17. As for the Daintree/Cape Tribulation scene, there are positive differences in agricultural areas due to plantation cycles, while the woodlands is a mixture of positive and negative changes in backscatter. It must be noted that many of the segments generated by the segmentation step occurred in agricultural regions. To eliminate these agricultural segments, a mask was first created using band 5 from the 1994 Landsat TM image, since the agricultural segments tended to be higher in band 5 than the rainforest areas. Once applied to the segmentation image, the remaining segments related to changes in rainforests and mangroves. The segments occurring in mangroves were most likely related to tidal effects, which have been shown to influence radar backscatter (e.g. Simard *et al.* 2000).

Further inspection was performed in more detail in the examples on the adjacent page:

Figure 18 shows a region that had undergone clearing between September 1994 and July 1996. Although it is a small area (approximately 175m*125m) it still is detectable in the JERS difference imagery (Figure 18c) and the segmentation extraction (Figure 18d). It must be emphasized that due to the speckle nature of radar, the difference image does appear noisy compared to the NDVI difference image. Therefore, only areas containing a group of negative pixels, such as the dark blue patch in Figure 18c, are likely candidates for deforestation.

Another example shown in Figure 19 demonstrates the identification of a more subtle change. The JERS is able to detect this change, however not all of it is extracted through the segmentation process. The NDVI difference image shows these areas more clearly. (Note how the region that was already cleared, shown by the white arrow in Figure 19d, has been successfully masked out as agriculture so does not show as change in the segmentation).

The JERS difference image also revealed some areas that did not appear to relate to rainforest clearing (Figure 20). It is unknown whether this is seasonal change or an artefact in the data, since it is not visible in the NDVI difference image. However, whilst not detected in the segmentation, the white arrow in Figure 20d shows a small region (approx 75m*75m) of rainforest reduction (detectable in the Landsat scenes) that shows up well in the JERS difference image.

It is important to note that deforestation is difficult to detect in JERS imagery when the replacement vegetation has already established significant biomass. Furthermore JERS data has a poor signal-to-noise ratio, hence low backscatter regions will appear noisy. Figure 21 shows an example where JERS data cannot discriminate between agricultural crops (outlined by the dashed line) and adjacent forest (dark in Figure 21a). The corresponding Landsat scene was acquired three months after the JERS scene (June 1994), so the crops may have possibly undergone change during the three-month period (such as harvesting), especially since they appear bare in the Landsat image. Even so, the crops in June 1994 cannot be distinguished from the adjacent forest.

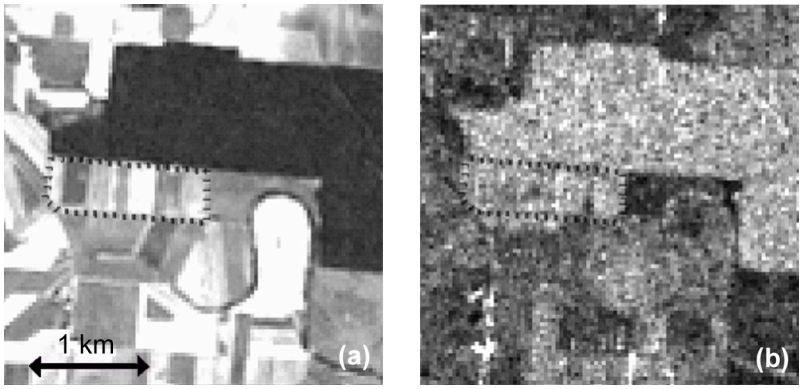

Figure 21. (a) September 1994 Landsat scene showing forest (dark grey) and cleared agricultural region (dashed outline). (b) June 1994 JERS scene of the same region.

CONCLUSIONS AND IMPLICATIONS FOR RAINFOREST MAPPING

JERS (SAR) imagery has been tested for its ability to detect rainforest clearing and was compared to similar products from optical Landsat TM imagery. Seasonal change was first analyzed to investigate its influence on the detected changes in SAR difference images. Some of the key implications of using SAR imagery for detecting rainforest clearing are:

- While optical satellite data has been shown to be effective in change detection, SAR images can be collected under any conditions at any time of the year hence it does provide a true year-round regional-scale monitoring tool for tropical regions.

- Selection of optimal SAR wavelengths would be recommended for detection of different types of change detection. L-Band radar systems appear to offer a good option for detection of both large-scale forest clearing, as well as more subtle seasonal changes in forest cover in tropical forest and forest/woodland conditions.

- SAR can be used as a surrogate for optical imagery for change detection, as long as caution is applied when interpreting the data. For JERS-1 data, regions as small as 10 pixels in size can be detected using visual interpretation, while more extensive regions (>100m*100m) can be automatically extracted. Due to the speckle nature of radar, areas of similar size, or smaller, to a pixel cannot be detected for change. It is only the areas consisting of a “clump” of negative pixels in a radar difference image that will indicate a realistic change. Attempts to extract thin linear regions of change is not recommended using JERS imagery, due to residual geo-location inaccuracies combined with speckle, which reduces the interpretability of the imagery.

- Radar data of finer resolution and shorter wavelengths is worth investigating further, including for use in mapping of selective logging. Technological limitations usually result in a compromise between number of available bands and spatial dimensions (resolution and extent), with airborne radar systems currently offering more information, but with smaller coverage. It is recommended that the authors continue investigations with existing airborne SAR (AIRSAR) data (5m pixels, C- L- and P-band with HH, VV and HV polarisations), to simulate expectations from current and future satellite radar systems for the Wet Tropics.

- Seasonal effects observed in the SAR imagery contribute additional information to optical image classification programs designed to distinguish between different forest types.

- To avoid inter-annual change detection, it is recommended that the radar data be acquired from the same time of year and climatic conditions to avoid confusion with seasonal effects.

- Even though the pre-masking of agricultural regions is recommended to avoid false-positives, rainforest clearing would only be detectable in SAR and optical imagery, when the cleared land contains relatively lower levels of biomass, or when forest successional stages have differing optical reflectance and/or radar backscatter properties. One solution to identifying only those regions that have changed from rainforest, is to geo-locate the imagery to existing map layers, such as the Stanton vegetation maps.

The JERS data in particular, is only single L-band SAR imagery, and has a relatively poor signal-to-noise ratio for more detailed applications. Therefore, further investigation is recommended into the use of more recently launched SAR systems, as well as using multiple-band and/or multiple polarization radar data for change detection analysis.

If this additional research further supports the suitability of SAR data as an indicator for rainforest clearing and fragmentation, additional indicators such as structural modifications will also be explored. Such indicators showing potential for SAR-based mapping are (from Phinn *et al.* 2001):

Indicator	**Status**
Land Cover Classes	Operational
Extent of clearing by stratification *(within land cover types: linear service corridors, inundation, spot clearings, boundary anomalies)*	Operational
Extent and severity of edge effects	Feasible
Structural modifications/forest health	Feasible
Extent of burnt area by spatial unit and assemblage *(within Webb-Tracey Communities and land cover types)*	Operational

It is recommended that WTMA continue with investigations along this line of technology, and also evaluate new processing approaches, so that it continues to meet State of Wet Tropics Indicator Monitoring needs using remote sensing as a regional mapping tool.

ACKNOWLEDGEMENTS

Funding for this project was provided by the Rainforest Cooperative Research Centre. JERS image data were provided by NASDA (National Space Development Agency of Japan).

REFERENCES

Archard, F. and Estreguil, C. (1995) Forest classification of southeast Asia using NOAA AVHRR data. *Remote sensing of Environment*, 54, 198-208.

Boyd, D.S., and Duane, W.J. (2001) Exploring spatial and temporal variation in middle infrared reflectance (at 3.75nm) measured from the tropical forest of west Africa. *International Journal of Remote Sensing*, 22(10), 1861-1878.

Castro, K.L., Sanchez-Azofeifa, G.A., and Rivard, B. (2003) Monitoring secondary tropical forests using space-borne data: implications for central America . *International Journal of Remote Sensing*, In press.

Ferrazzoli, P., Paloscia, S., Pampaloni, P., Schiavon, G., Sigismondi, S., and Solimini, D. (1997) The potential of multifrequency polarimetric SAR in assessing agricultural and arboreous biomass. *IEEE Transactions on Geoscience and Remote Sensing*, 35(1), 5-16.

French, N.H.F, Kasischke, E.S, Bourgeau-Chavez L.L, and Harrell, P.A. (1996) Sensitivity of ERS-1 SAR to variations in soil water in fire-disturbed boreal forest ecosystems. *International Journal of Remote Sensing*, 17(15), 3037-3053.

Griffiths, G.H., and Wooding, M.G. (1996) Temporal monitoring of soil moisture using ERS-1 SAR data. *Hydrological Processes*, 10(9), 1127-1138.

Hill, M.J., Donald, G.E., and Vickery, P.J. (1999) Relating radar backscatter to biophysical properties of temperate perennial grassland. *Remote Sensing of Environment*, 67, 15-31.

Kasischke, E.S., Christensen, N.L., and Bourgeau-Chavez, L.L., (1995) Correlating radar backscatter with components of biomass in Loblolly pine forests. *IEEE Transactions on Geoscience and Remote Sensing*, 33(3), 643-659.

Lu, D., Mausel, P., Brondizio, E., and Moran, E. (2002) Assessment of atmospheric correction methods for Landsat TM data applicable to Amazon basin LBA research. *International Journal of Remote Sensing*, 23(13), 2651-2671.

Lucas, R.M., Held, A., and Phinn, S. (2002) Tropical Forests. In: *Manual of Remote Sensing, Volume 4, Remote Sensing for Natural Resource Assessment*. Ustin, S.(eds). American Society for Photogrammetry and Remote Sensing, Bethesda, Maryland. In press 03/02.

Lucas,R.M., Honzak,M., Curran,P.J., Foody,G.M., and Nguele,D.T. (2000) Characterizing tropical forest regeneration in Cameroon using NOAA AVHRR data. *International Journal of Remote Sensing*, 21(15), 2831-2854.

Luckman, A., Baker, J., Kuplich, T.M., Yanasse, C.C.F, and Frery, A.C. (1997) A study of the relationship between radar backscatter and regenerating tropical forest biomass for spaceborne SAR instruments. *Remote Sensing of Environment*, 60, 1-13.

Mayaux,P., and Lambin,E.F. (1997) Tropical forest area measured from global land-cover classifications: inverse calibration models based on spatial textures. *Remote sensing of Environment*, 59, 29-43.

Phinn, S., Stanford, M., Held, A., Ticehurst, C.J. (2001) *Evaluating the feasibility of remote sensing for monitoring State of the Wet Tropics environmental indicators*. Cooperative Research Centre for Tropical Rainforest Ecology and Management, Cairns. (74 pages).

Rosenqvist, A. (2001) NASDA (National Space Development Agency), Japan's government space agency.

Rosenqvist, A., Shimada,M., Chapman,B., Freeman.A., De Grandi,G., Saatchi,S., and Rauste,Y. (2000) The Global Rain Forest Mapping project – a review. *International Journal of Remote Sensing*, 21(6&7), 1375-1387.

Saatchi, S.S., and Moghaddam, M. (2000) Estimation of crown and stem water content and biomass of boreal forest using polarimetric SAR imagery. *IEEE Transactions on Geoscience and Remote Sensing*, 38(2), 697-709.

Shimada, M. (1998) *Users guide to NASDA's SAR products*, Earth Observation research center, National Space Development Agency of Japan, 24pp.

Simard, M., Saatchi, S.S., and De Grandi, G. (2000) The use of decision tree and multiscale texture for classification of JERS-1 SAR data over tropical forest. *IEEE Transactions on Geoscience and Remote Sensing*, 38(5), 2310-2321.

Skole, D.L., and Tucker, C.J. (1993) Tropical deforestation and habitat fragmentation in the Amazon: Satellite data from 1978 to 1988. *Science*, 260, 1905-1910.

Tucker, C.J. (1979) Red and photographic infrared linear combinations for monitoring vegetation. *Remote Sensing of Environment*, 8, 127-150.

Webb, L.J. (1968) Environmental relationships of the structural types of Australian rain forest vegetation. *Ecology*, 49(2), 296-311.

APPENDIX A

Appendix A contains a Radar Flyer which is a black and white version of an excerpt from the September 2002 Remote Sensing Primer and Satellite Image Brochure compiled and written by Geoimage Pty Ltd.

Radar Imagery

Microwave sensing covers that part of the electromagnetic spectrum between 1cm to 1m in wavelength. Because of their long wavelengths compared to the visible and infrared parts of the spectrum, microwaves have the important property that they can penetrate through cloud cover, haze, dust and all but the heaviest rainfall as they are not affected by atmospheric scattering. This property allows detection of microwave energy under almost all weather and environmental conditions so that data can be collected at any time. Although microwave sensing encompasses both passive and active systems, in the passive systems, the signal magnitudes are very small and only used in meteorology, hydrological and oceanographic applications.

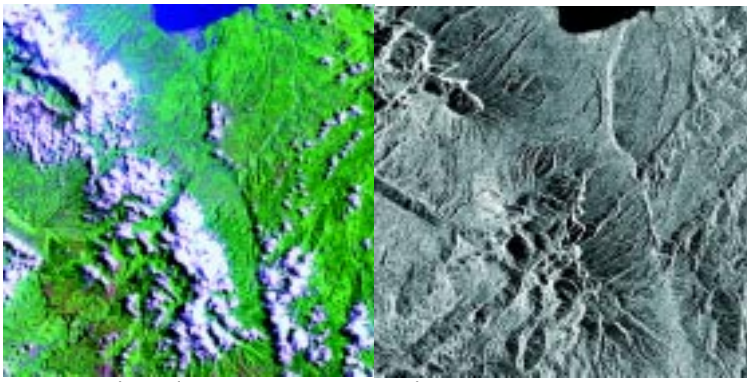

LANDSAT Thematic Mapper Radar Image ®RADARSAT 1997

Active microwave sensors provide their own source of microwave radiation to illuminate the target. The main imaging type is RADAR which is an acronym for **RA**dio **D**etection **A**nd **R**anging which essentially characterizes the function and operation of a radar sensor. The sensor transmits a microwave (radio) signal towards the target and detects the backscattered portion of the signal. The strength of the backscattered signal is measured to discriminate between different targets and the time delay between the transmitted and reflected signals determines the distance (or range) to the target.

The two primary advantages of radar are the all-weather and day or night imaging. It is also important to understand that, because of the fundamentally different way in which an active radar operates compared to the passive optical sensors, a radar image is quite different from and has special properties unlike images acquired in the visible and infrared portions of the spectrum. Because of these differences, radar and optical data can be complementary to one another as they offer different perspectives of the Earth's surface providing different information content.

RADAR BASICS

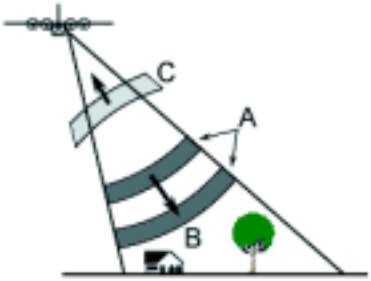

A radar is essentially a ranging or distance measuring device. It consists fundamentally of a transmitter, a receiver, an antenna, and an electronics system to process and record the data. The transmitter generates successive short bursts (or pulses) of microwaves (A) at regular intervals which are focused by the antenna into a beam (B). The radar beam illuminates the surface obliquely at a right angle to the motion of the platform. The antenna receives a portion of the transmitted energy reflected (or backscattered) from various objects within the illuminated beam (C). By measuring the time delay between the transmission of a pulse and the reception of the backscattered "echo" from different targets, their distance from the radar and thus their location can be determined. As the sensor platform moves forward, recording and processing of the backscattered signals builds up a two-dimensional image of the surface.

While we have characterized electromagnetic radiation in the visible and infrared portions of the spectrum primarily by wavelength, microwave portions of the spectrum are often referenced according to both wavelength and frequency. The microwave region of the spectrum is quite large, relative to the visible and infrared, and there are several wavelength ranges or bands commonly used. These were given code letters during World War II that remain to this day.

* Ka, K, and Ku bands: very short wavelengths used in early airborne radar systems but uncommon today.
* X-band: used extensively on airborne systems for military reconnaissance and terrain mapping.
* C-band: common on many airborne research systems (CCRS Convair-580 and NASA AirSAR) and spaceborne systems (including ERS-1 and 2 and RADARSAT).
* S-band: used on board the Russian ALMAZ satellite.
* L-band: used onboard American SEASAT and Japanese JERS-1 satellites and NASA airborne system.
* P-band: longest radar wavelengths, used on NASA experimental airborne research systems.

When discussing microwave energy, the polarization of the radiation is also important. Polarization refers to the orientation of the electric field (recall the definition of electromagnetic radiation from Chapter 1). Most radars are designed to transmit microwave radiation either horizontally polarized (H) or vertically polarized (V). Similarly, the antenna receives either the horizontally or vertically polarized backscattered energy, and some radars can transmit and receive both. These two polarization states are designated by the letters H for horizontal, and V, for vertical. Thus, there can be four combinations of both transmit and receive polarizations as follows:

• HH - for horizontal transmit and horizontal receive,
• VV - for vertical transmit and vertical receive,
• HV - for horizontal transmit and vertical receive, and
• VH - for vertical transmit and horizontal receive.

The first two polarization combinations are referred to as like-polarized because the transmit and receive polarizations are the same. The last two combinations are referred to as cross-polarized because the transmit and receive polarizations are opposite of one another.

VIEWING GEOMETRY

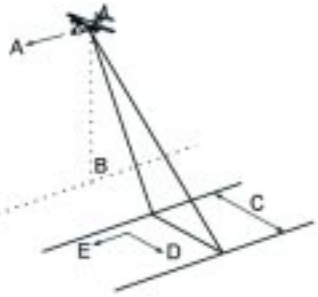

The imaging geometry of a radar system is different from the framing and scanning systems commonly employed for optical remote sensing. Similar to optical systems, the platform travels forward in the flight direction (A) with the nadir (B) directly beneath the platform. The microwave beam is transmitted obliquely at right angles to the direction of flight illuminating a swath (C) which is offset from nadir. Range (D) refers to the across-track dimension perpendicular to the flight direction, while azimuth (E) refers to the along-track dimension parallel to the flight direction. This side-looking viewing geometry is typical of imaging radar systems (airborne or spaceborne).

The portion of the image swath closest to the nadir track of the radar platform is called the near range while the portion of the swath farthest from the nadir is called the far range. The incidence angle is the angle between the radar beam and ground surface which increases, moving across the swath from near to far range. The look angle is the angle at which the radar "looks" at the surface. In the near range, the viewing geometry may be referred to as being steep, relative to the far range, where the viewing geometry is shallow. At all ranges the radar antenna measures the radial line of sight distance between the radar and each target on the surface. This is the slant range distance. The ground range distance is the true horizontal distance along the ground corresponding to each point measured in slant range.

Unlike optical systems, a radar's spatial resolution is a function of the specific properties of the microwave radiation and geometrical effects. In the case of a Real Aperture Radar (RAR) e.g. Side-Looking Airborne Radar, a single transmitted pulse and the backscattered signal are used to form the image. In this case, the range or across track resolution is dependent on the effective length of the pulse in the slant range direction and the azimuth or along-track resolution is dependent on the width of the illumination in the azimuth direction. Since the microwave beam widens with distance from the antenna, the azimuth resolution increases with range distance in RAR.This problem is overcome with most airborne and spaceborne radars using a system called synthetic aperture radar or SAR which achieves a uniform fine azimuth resolution across the entire imaging swath. This is achieved by shorter pulse lengths, increased antenna length and by the use of special techniques for recording and processing the backscatter echoes.

RADAR IMAGE DISTORTION

As with all remote sensing systems, the viewing geometry of a radar results in certain geometric distortions of the resultant imagery. However, there are key differences for radar imagery which are due to the side-looking viewing geometry, and the fact that the radar is fundamentally a distance measuring device (i.e. measuring range). Slant-range scale distortion occurs because

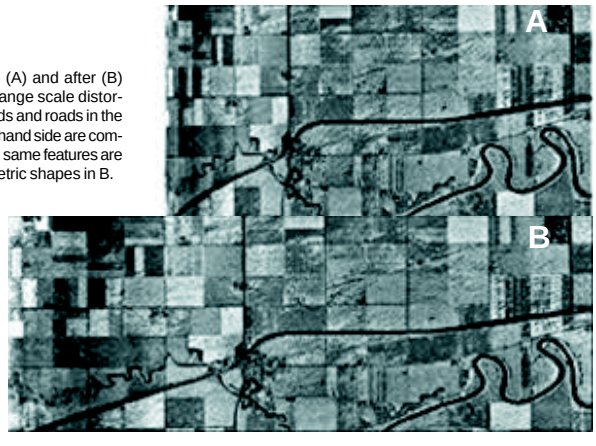

Radar image before (A) and after (B) correction for slant-range scale distortion. Note that the fields and roads in the near range on the left hand side are compressed in A while the same features are in their correct geometric shapes in B.

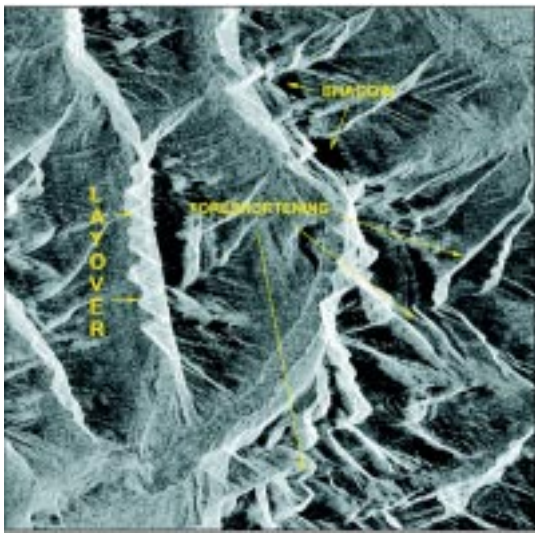

Layover, foreshortening and shadow with SAR imagery (RADARSAT-1 Standard beam position 1. 20x20km area. ©Canadian Space Agency 1996. Used courtesy of RADARSAT International Inc.

the radar is measuring the distance to features in slant-range rather than the true horizontal distance along the ground. This results in a varying image scale, moving from near to far range with targets in the near range appearing compressed relative to the far range. Corrections to convert the image to a ground-range display are easily applied.

Similar to the distortions encountered when using cameras and scanners, radar images are also subject to geometric distortions due to relief displacement. As with scanner imagery, this displacement is one-dimensional and occurs perpendicular to the flight path. However, the displacement is reversed with targets being displaced towards, instead of away from the sensor. Radar foreshortening and layover are two consequences resulting from relief displacement.

When the radar beam reaches the base of a tall feature tilted towards the radar (e.g. a mountain) before it reaches the top, foreshortening will occur. Again, because the radar measures distance in slant-range, the slope (A to B) will appear compressed and the length of the slope will be represented incorrectly (A' to B'). Depending on the angle of the hillside or mountain slope in relation to the incidence angle of the radar beam, the severity of foreshortening will vary. Maximum foreshortening occurs when the radar beam is perpendicular to the slope such that the slope, the base, and the top are imaged simultaneously (C to D). The length of the slope will be reduced to an effective length of zero in slant range (C'D'). This figure shows a radar image of steep mountainous terrain with severe foreshortening effects. The foreshortened slopes appear as bright features on the image.

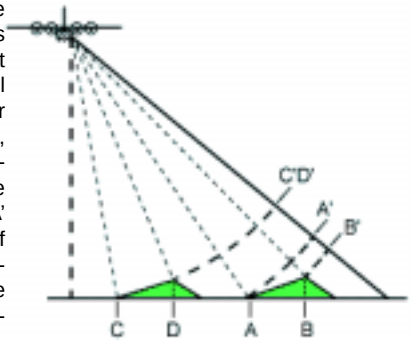

Layover occurs when the radar beam reaches the top of a tall feature (B) before it reaches the base (A). The return signal from the top of the feature will be received before the signal from the bottom. As a result, the top of the feature is displaced towards the radar from its true position on the ground, and "lays over" the base of the feature (B' to A'). Layover effects on a radar image look very similar to effects due to foreshortening. As with foreshortening, layover is most severe for small incidence angles, at the near range of a swath, and in mountainous terrain.

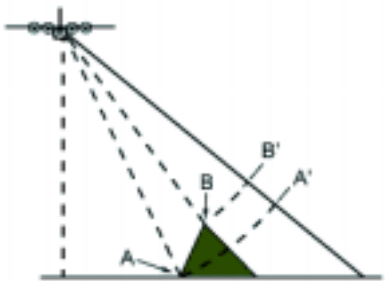

Both foreshortening and layover result in radar shadow. Radar shadow occurs when the radar beam is not able to illuminate the ground surface. Shadows occur in the down range dimension (i.e. towards the far range), behind vertical features or slopes with steep sides. Since the radar beam does not illuminate the surface, shadowed regions will appear dark on an image as no energy is available to be backscattered. As incidence angle increases from near to far range, so will shadow effects as the radar beam looks more and more obliquely at the surface. This image illustrates radar shadow effects on the right side of the hillsides which are being illuminated from the left.

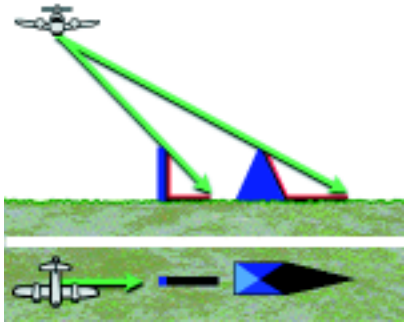

TARGET INTERACTION AND IMAGE APPEARANCE

The brightness of features in a radar image is dependent on the portion of the transmitted energy that is returned back to the radar from targets on the surface and this is dependent on how the radar energy interacts with the surface. This interaction is a function of the characteristics of the radar system (frequency, polarization, viewing geometry, etc.) as well as the characteristics of the surface (landcover type, topography, relief, etc.). We can group these characteristics into three areas which fundamentally control radar energy/target interactions. They are:

• Surface roughness of the target

The surface roughness of a feature controls how the microwave energy interacts with that surface or target and is generally the dominant factor in determining the tones seen on a radar image. Surface roughness refers to the average height variations in the surface cover from a plane surface, and is measured on the order of centimetres. Whether a surface appears rough or smooth to a radar depends on the wavelength and incidence angle. Simply put, a surface is considered "smooth" if the height variations are much smaller than the radar wavelength. When the surface height variations begin to approach the size of the wavelength, then the surface will appear "rough". Thus, a given surface will appear rougher as the wavelength becomes shorter and smoother as the wavelength becomes longer. A smooth surface (A) causes specular or mirror like reflection of the incident energy (generally away from the sensor) and thus only a small amount of energy is returned to the radar. This results in smooth surfaces appearing as darker toned areas on an image. A rough surface (B) will scatter the energy approximately equally in all directions (i.e. diffusely) and a significant portion of the energy will be backscattered to the radar. Thus, rough surfaces will appear lighter in tone on an image.

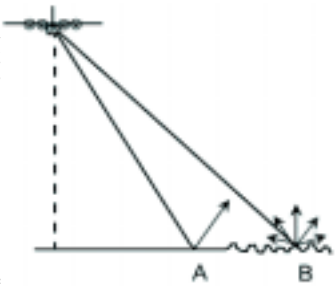

• Radar viewing and surface geometry relationship

The **local incidence angle** is an important concept related to target interaction and image appearance. It is the angle between the radar beam and a line perpendicular to the slope at the point of incidence. Thus, local incidence angle takes into account the local slope of the terrain in relation to the radar beam. With flat terrain, the local incidence angle is the same as the look angle of the radar. However for areas of strong relief, slopes facing towards the radar will have small local incidence angles, causing relatively strong backscattering and resulting in a bright-toned appearance in an image.

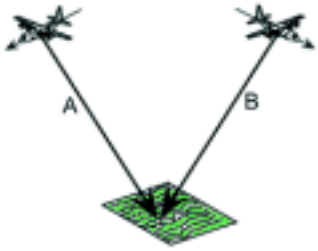

The **look direction** or aspect angle of the radar describes the orientation of the transmitted radar beam relative to the direction or alignment of linear features on the surface, such as agricultural crops or mountain ranges. If the look direction is close to perpendicular to the orientation of the feature (A), then a large portion of the incident energy will be reflected back to the sensor and the feature will appear as a brighter tone. If the look direction is more oblique in relation to the feature orientation (B), then less energy will be returned to the radar and the feature will appear darker in tone. Look direction is important for enhancing the contrast between features in an image .eg. to maximize the reflectivity of linear features with minimal relief.

• Moisture content and electrical properties of the target

The presence (or absence) of moisture affects the electrical properties of an object or medium and this influences the absorption, transmission, and reflection of microwave energy. Generally, reflectivity (and image brightness) increases with increased moisture content. For example, surfaces such as soil and vegetation cover will appear brighter when they are wet than when they are dry.

RADAR IMAGE PROPERTIES

All radar images appear with some degree of what we call radar speckle. This appears as a grainy "salt and pepper" texture in an image and this is caused by random constructive and destructive interference from the multiple scattering returns that occur within each resolution cell. Speckle is essentially a form of noise which degrades the quality of an image and may make interpretation (visual or digital) more difficult. Thus, it is generally desirable to reduce speckle prior to interpretation and analysis. Speckle reduction can be achieved either by multi-look processing, or by spatial filtering.

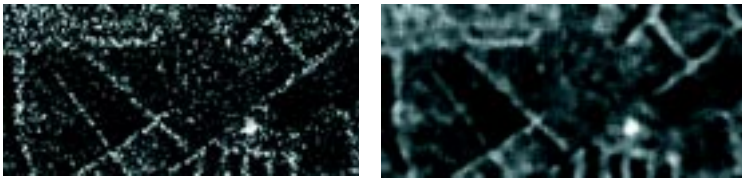
Speckle reduction using spatial filtering

DEMS FROM RADAR IMAGERY

Two methods are currently employed to produce digital elevation models from Radar imagery.

The first is stereo radar or radargrammetry which is similar in concept to stereo mapping using aerial photography. Stereo radar image pairs are acquired covering the same area, but with different look/ incidence angles, or opposite look directions. Unlike aerial photos where the displacement is radially outward from the nadir point directly below the camera, radar images show displacement only in the range direction. Stereo pairs taken from opposite look directions (i.e. one looking north and the other south) may show significant contrast and may be difficult to interpret visually or digitally. In mountainous terrain, this will be even more pronounced as shadowing on opposite sides of features will eliminate the stereo effect.

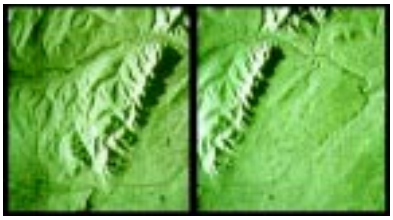

Example of same side stereo radar images

The second more advanced method is called interferometry. Interferometry relies on being able to measure a property of electromagnetic waves called phase. Suppose we have two waves with the exact same wavelength and frequency travelling along in space, but the starting point of one is offset slightly from the other. The offset between matching points on these two waves (A) is called the phase difference. Interferometric systems use two antennas, separated in the range dimension by a small distance, both recording the returns from each resolution cell. The two antennas can be on the same platform (as with some airborne SARs), or the data can be acquired from two different passes with the same sensor, as has been done with both airborne and satellite radars. By measuring the exact phase difference between the two returns (A), the path length difference can be calculated to an accuracy that is on the order of the wavelength (i.e centimetres). Knowing the position of the antennas with respect to the Earth's surface, the position of the resolution cell, including its elevation, can be determined. The phase difference between adjacent resolution cells, is illustrated in this interferogram, where colours represents the variations in height. The information contained in an interferogram can be used to derive topographic information and produce three-dimensional imagery of terrain height.

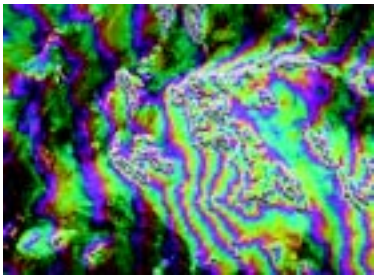

AIRBORNE AND SPACEBORNE RADARS

Like other remote sensing systems, an imaging radar sensor may be carried on either an airborne or spaceborne platform. Depending on the use of the prospective imagery, there are trade-offs between the two types of platforms. Regardless of the platform used, a significant advantage of using a Synthetic Aperture Radar (SAR) is that the spatial resolution is independent of platform altitude. Thus, fine resolution can be achieved from both airborne and spaceborne platforms.

Airborne and Spaceborne systems which have contributed significantly to our understanding of Radar and its applications are-

The Convair-580 C/X SAR system developed and operated by the Canada Centre for Remote Sensing was a workhorse for experimental research into advanced SAR applications in Canada and around the world, particularly in preparation for satellite-borne SARs.

The Sea Ice and Terrain Assessment (STAR) systems operated by Intera Technologies Limited of Calgary, Alberta, Canada, (later Intermap Technologies) were among the first SAR systems used commercially around the world. Both STAR-1 and STAR-2 operate at X-band (3.2 cm) with HH polarization in two different resolution modes.

The United States National Aeronautics and Space Administration (NASA) has been at the forefront of multi-frequency, multi-polarization synthetic aperture radar research for many years. The Jet Propulsion Laboratory (JPL) in California has operated various advanced systems on contract for NASA. The AirSAR system is a C-, L-, and P-band advanced polarimetric SAR which can collect data for each of these bands at all possible combinations of horizontal and vertical transmit and receive polarizations (i.e. HH, HV, VH, and VV). Data from the AirSAR system can be fully calibrated to allow extraction of quantitative measurements of radar backscatter. Spatial resolution of the AirSAR system is in the order of 12 metres in both range and azimuth. Incidence angle ranges from zero degrees at nadir to about 70 degrees at the far range. This capability to collect multi-frequency, multi-polarization data over such a diverse range of incidence angles allows a wide variety of specialized research experiments to be carried out.

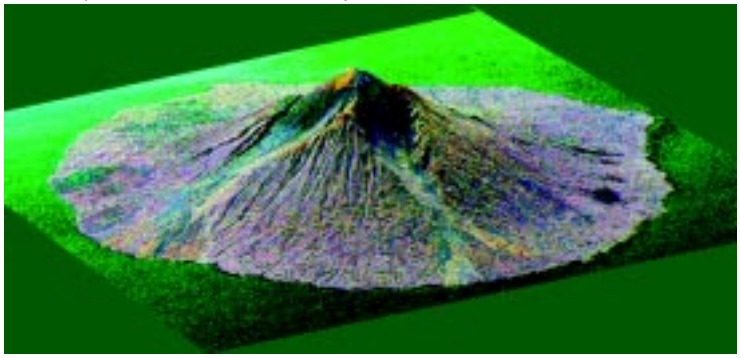

AirSar perspective view of Manam Volcano, PNG. Images Courtesy Jet Propulsion Laboratory. Copyright © California Institute of Technology, Pasadena, Ca. All rights reserved.

With the advances and success of airborne imaging radar, satellite radars were the next logical step to complement the optical satellite sensors in operation. SEASAT, launched in 1978, was the first civilian remote sensing satellite to carry a spaceborne SAR sensor. The SAR operated at L-band (23.5 cm) with HH polarization. The viewing geometry was fixed between nine and 15 degrees with a swath width of 100 km and a spatial resolution of 25 metres. This steep viewing geometry was designed primarily for observations of ocean and sea ice, but a great deal of imagery was also collected over land areas. However, the small incidence angles amplified foreshortening and layover effects over terrain with high relief, limiting its utility in these areas. Although the satellite was only operational for three months, it demonstrated the wealth of information (and the large volumes of data!) possible from a spaceborne radar. Since 1991, four spaceborne SARS, ERS1, ERS2, JERS1 and RADARSAT1 have provided global coverage and are described in detail on Pages 29 to 32.

The **Shuttle Radar Topography Mission** (SRTM) is a joint project of NASA and the Department of Defence's National Imagery and Mapping Agency (NIMA). Using the Spaceborne Imaging Radar (SIR-C) and X-Band Synthetic Aperture Radar (X-SAR) hardware that flew twice on Space Shuttle Endeavour in 1994, SRTM collected data in a single shuttle flight in February 2000. The SIR-C/X-SAR is a multifrequency, multipolarization imaging radar system was complemented by additional C-Band and X-Band antennas located at the end of a 60-metre-long mast which deployed from the shuttle after reaching orbit. This configuration produced single-pass interferometry and SRTM acquired data with 225 kilometre swaths, imaging all of the Earth's land surface between 60 degrees north and 50 degrees south during the mission. Data from the mission is still being processed however it is expected that a DEM will be available by mid 2004 at a resolution of 30m over the US and 90m over the rest of the world. The absolute horizontal and vertical accuracy will be 20metres and 16metres respectively. A C-Band radar image mosaic will also be produced at 30metres resolution.

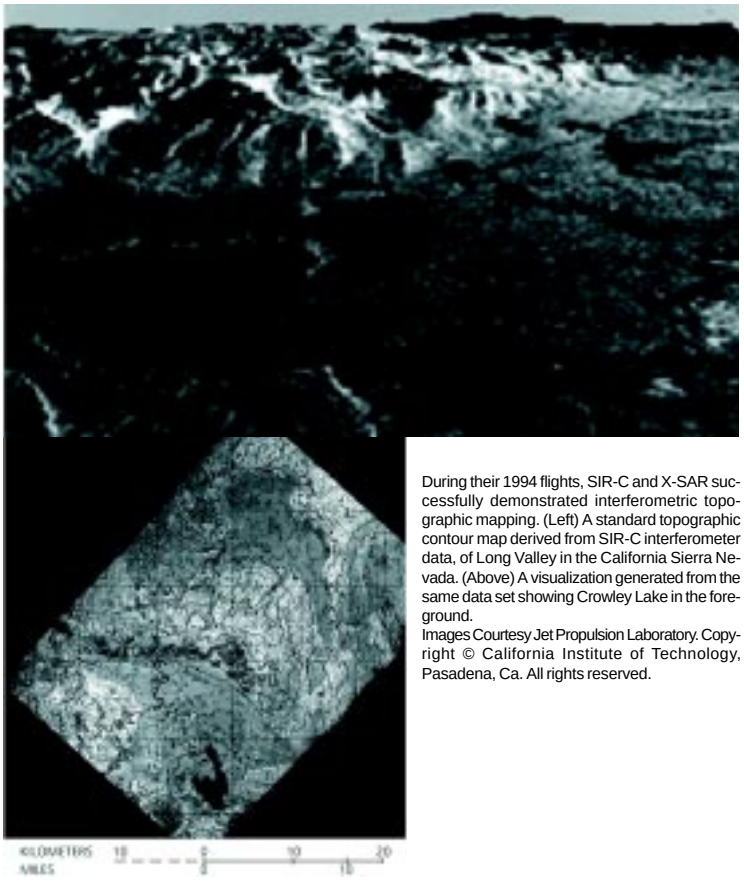

During their 1994 flights, SIR-C and X-SAR successfully demonstrated interferometric topographic mapping. (Left) A standard topographic contour map derived from SIR-C interferometer data, of Long Valley in the California Sierra Nevada. (Above) A visualization generated from the same data set showing Crowley Lake in the foreground.

Images Courtesy Jet Propulsion Laboratory. Copyright © California Institute of Technology, Pasadena, Ca. All rights reserved.

The Canadian Centre for Remote Sensing have a brilliant on line remote sensing tutorial on their web site and their permission to use parts of the Microwave section on Pages 16, 17, 18 and 21 is gratefully acknowledged. This tutorial can be found at http://www.ccrs.nrcan.gc.ca.